Draft version August 30, 2020
Typeset using LaTeX **twocolumn** style in AASTeX63

Molecular Gas Toward the Supermassive Black Hole Sagittarius A*

S. Cronin,[1] J. Ott,[2] D. Meier,[2,3] and B. Svoboda[2]

[1] *The Ohio State University, Columbus, OH*
[2] *National Radio Astronomy Observatory, Socorro, NM*
[3] *New Mexico Institute of Mining and Technology, Socorro, NM*

ABSTRACT

We present $\sim 1''$ resolution ALMA observations of molecular clouds along the line-of-sight to Sgr A*. We report absorption detections that lead to the placement of 6 velocity features in either the spiral arms, bar, or Galactic Center (GC). We aimed at 18 high-energy molecular transitions in hopes of picking up clouds in the circumnuclear disk (CND) to study the environment around Sgr A*. For each velocity feature, or cloud, we analyzed its kinematics, chemistry, excitation, and CO isotopologues in order to locate it along our line-of-sight. We place 2 clouds in the Central Molecular Zone (CMZ), both perhaps in the 100 pc ring and possibly related to the +20 km s^{-1} and +50 km s^{-1} molecular clouds. We designate 3 clouds as being in the Galactic Disk, and kinematics suggest they are in the inner Galactic Disk, perhaps around the 3 kpc arm of the bar. We are unable to determine the properties of one of our clouds and thus are not able to speculate about its location. This is due to saturated CO isotopologue data at its velocity. We do not have a current candidate for CND material, though we hope to unveil a candidate by looking at emission features in a future study.

1. INTRODUCTION

Supermassive black holes (SMBHs) are typically far away in other galaxies. Their spheres of influence should be dominated by strong tidal forces, high energy injected by an accretion disk, and energetic inflows and outflows. These spheres of influence are relatively small, and so the environments around SMBHs are not very well understood. The nearest SMBH is Sagittarius A* (Sgr A*), which lies ∼8.178 kpc away at the center of our Galaxy (Gravity Collaboration et al. 2019).

Certain molecular lines are known tracers of the physical conditions of molecular gas, such as shocks, ionization, and density. Thus, probing the chemistry of the gas around Sgr A* provides key insight into the physics of the immediate environment around the SMBH. We can then use Sgr A* as a reference for comparisons with other SMBHs in order to develop a deeper understanding of their turbulent environments.

Sgr A* lies deep within the inner 500 pc of the Galaxy called the Central Molecular Zone (CMZ). The CMZ is a hot, dense region that is luminous at both radio and infrared frequencies (Morris & Serabyn 1996). The central ∼100 pc of the CMZ forms an inclined figure eight-like structure called the 100 pc ring, within which the Sgr A complex and well-known massive molecular clouds (e.g. the +20 km s^{-1} and +50 km s^{-1} clouds) reside (Molinari et al. 2011).

In the very vicinity of Sgr A*, one can find another ring-like structure known as the Circumnuclear Disk (CND), which is part of the Sgr A complex. The CND has a radius of ∼2 pc, and contains clumpy, hot, and dense molecular material (Morris & Serabyn 1996 and references therein).

In this report, we present an absorption study toward Sgr A* that reveals a number of molecular clouds. These clouds may include gas in the SMBH's sphere of influence inside and around the CND. However, our data also contains clouds that are far out in the Galactic Disk or somewhere in the CMZ, but not necessarily in the immediate environment of the Galaxy's SMBH. Therefore, we must properly place the molecular material in the absorption spectra along our line-of-sight to reveal potential candidates for CND molecular gas.

2. DATA

We conducted observations using the Atacama Large Millimeter/submillimeter Array (ALMA). We observed Sgr A* with the 12 meter array (α = $17^h45^m40.041^s$, δ = -29°00′28.118″) as part of Cycle 0 project 2012.1.00628.T (PI: J. Ott). The collected data were calibrated by the North American ALMA NAASC. We used ALMA band 6 and band 7 to target the rest frequencies of specific molecules and molecular transitions. Table 1 is a collection of each transition we aimed at and its corresponding ALMA band and rest frequency

in GHz. These molecular lines are relatively high-energy transitions at millimeter wavelengths, which are great at tracing warm clouds. For absorption, warm molecular gas has a temperature above that of the CMB, or ∼2.7 K. Thus, our observations should have been well-tailored toward picking up clouds not only in the GC, but also somewhere in and around the CND.

We obtained a spectral resolution of 244.141 kHz over a bandwidth of 468.75 MHz. Velocity resolution ranges are 0.317 km s^{-1} − 0.335 km s^{-1} and 0.278 km s^{-1} − 0.281 km s^{-1} for ALMA band 6 data, and 0.212 km s^{-1} − 0.221 km s^{-1} for ALMA band 7 data. The total observation time was ∼3 hours.

3. RESULTS

We image and deconvolve the data using CASA. We convolve the maps to a common spatial resolution (beamsize) of 1.096″. Figure 1 features channels from our ^{12}CO(3-2) data cube that visualize continuum and line emission as well as line absorption. We see total absorption in our ^{12}CO cubes. This occurs when the clouds along the line-of-sight become completely opaque.

3.1. *Spectra in Jy bm^{-1}*

From the data cubes, we extract spectral profiles in Jy bm^{-1} (Figure 2). The continuum flux for Sgr A* appears to stay approximately constant with a frequency of ∼3.2 Jy bm^{-1}.

There are a variety of spectral features in these profiles, including emission, which is most notably found in the ^{12}CO, ^{13}CO, and CS spectra. However, the aim of this REU project was to study absorption features, and we will analyze emission in a larger study.

For each spectrum, we flag single-channel spikes as artifacts because features less than a single channel wide are unphysical to observe along this line-of-sight. We also trim the spectra to only show the features that correspond to the relevant molecular line. This was done by identifying isolated features in an uncontaminated cube (H_2CO), then using its velocity to identify additional spectral lines within the other cubes. For instance, CH_3OH and SO have rest frequencies close enough together that they are in the same spectral window. Therefore, the same two spikes appear in both the full CH_3OH and SO spectra. We determine that the ∼10 km s^{-1} absorption feature in each of these spectra are the actual detections of the respective molecule, following the shift we see for H_2CO. We then separate out the peaks from the spectra.

There are clear absorption detections of all CO isotopologues from Table 1 in the flux density spectra. Furthermore, the presence of lines other than CO isotopologues means certain velocity features are chemically rich, hinting at their physical conditions and possible placements along our line-of-sight. C_2H, CH_3OH, and CS are additional lines clearly detected in the most chemically-rich velocity features, the latter of which is a known dense gas tracer. Other molecular lines are also great at probing specific physical conditions of gas. Comparing CO isotopologues with ^{12}CO transitions can characterize the opacity of certain velocity features. Calculating ^{12}CO(3-2)/^{12}CO(2-1) ratios can also establish the excitation of these clouds. Clear detections of these molecular lines span a velocity range of roughly −150 km s^{-1} to +150 km s^{-1}.

There are possible weak features of C^{15}N and N_2D^+ at some velocities, though further investigation is needed. C^{15}N is comparable to C_2H as a PDR tracer, making it interesting that C^{15}N does not have clear detections like C_2H.

There are some absorption features that we are currently unable to identify with the appropriate molecular lines. The most notable of these are two absorption features seen in the NH_2D spectrum. We expect a separation of ∼36.8 km s^{-1} for the corresponding o-NH_2D and p-NH_2D pair, but instead see a separation of ∼160 km s^{-1} between the two bright features present in the spectrum. It is possible that the larger feature at 109.75 km s^{-1} in the o-NH_2D spectrum (146.25 km s^{-1} for p-NH_2D) is unrelated to NH_2D and is an unidentified molecule in the same spectral window. This would make the smaller absorption feature either o-NH_2D or p-NH_2D with a different spectral feature being its corresponding ortho or para pair. More investigation is needed with the NH_2D spectrum in order to fully understand these bright absorption features.

It is difficult to determine if there is a detection of HNCO, as this spectrum has a baseline issue due to the presence of atmospheric lines. We do not include HNCO in Figure 2.

Finally, there is no detection of SiO in the spectral profiles, also excluding it from Figure 2. This is a surprising result because we expect to find cases of shocked gas in the turbulent GC.

3.2. *Spectra in Opacity Space*

We next convert our spectra from flux density to opacity using

$$\tau = -\ln\left(1 - \frac{T_L}{T_C}\right), \tag{1}$$

where $T_L = T_{measured} - T_C$ and T_C is the continuum flux (Figure 3). For instances of emission, τ is negative, as defined in the above equation. Any $\tau < \sigma$ we set to

Table 1: Summary of the molecular lines we aimed at along the line-of-sight toward Sgr A*.

Molecule	Transition	Rest Freq. (GHz)	RMS (Jy bm^{-1})	ALMA Band
H_2CO	$3_{2,1}$-$2_{2,0}$	218.760070	0.005205	6
$C^{18}O$	$2-1$	219.560360	0.007819	6
$C^{15}N$	$J=\frac{3}{2}-\frac{1}{2}, N=2-1, F=1-0$	219.70874	0.007819	6
$C^{15}N$	$J=\frac{3}{2}-\frac{1}{2}, N=2-1, F=2-1$	219.72249	0.007819	6
^{12}CO	$2-1$	230.538000	0.013602	6
N_2D^+	$3-2$	321.321860	0.00557	6
C_2H	$J=\frac{7}{2}-\frac{5}{2}$, $N=3-2$, $F=4-3$	262.004260	0.006075	6
C_2H	$J=\frac{7}{2}-\frac{5}{2}$, $N=3-2$, $F=3-2$	262.0648433	0.006075	6
SO	6_7-5_6	261.84368	0.006075	6
CH_3OH	$2_{1,1}$-$1_{0,1}$	261.80568	0.006075	6
HNCO	$12_{0,12}$-$11_{0,11}$	263.748630	0.0068	6
$H^{13}CO^+$	$3-2$	260.25534	0.00538	6
SiO	$6-5$	260.518020	0.00538	6
CS	$7-6$	342.882860	0.00538	7
^{12}CO	$3-2$	345.795990	0.014321	7
^{13}CO	$3-2$	330.587965	0.00838	7
o-NH_2D	$1_{0,1}0$-$0_{0,0}$, $N=2-1$	332.78189	0.007362	7
p-NH_2D	$1_{0,1}0$-$0_{0,0}$, $N=2-1$	332.82251	0.007362	7

equal to σ, where σ is the RMS of the data cube (see Table 1). We also use a σ cutoff when absorption is zero to avoid τ being infinite. We then trim each spectrum to only showcase the relevant spectral features.

The ^{12}CO spectra contain many "flat tops," which correspond to complete absorption. In these cases, the clouds along our line-of-sight are completely opaque and our data becomes saturated, with the highest opacity values of $\tau > 5$. Thus, detections where there are flat tops are not as clear as, for example, the bright detection at 10.75 km s^{-1} in the ^{12}CO and ^{13}CO spectra.

After analyzing the spectra in both flux density and opacity space, we see that there is pronounced absorption at -135 km s^{-1}, -55 km s^{-1}, -33 km s^{-1}, -13.25 km s^{-1}, $+10.75$ km s^{-1}, and $+42.5$ km s^{-1}. We now aim to place these clouds along our line-of-sight.

3.3. *Cloud Identification*

We next analyze the chemistry and kinematics of these clouds. We also calculate CO isotopologue ratios to study their excitation and possible Galactocentric distance. The combination of these factors, plus support from the literature, allows us to draw reasonable conclusions on the locations of these clouds along our line-of-sight. Table 2 is a summary of each cloud's CO isotopologue ratios, chemistry, and kinematics that we outline in the following three sections.

3.3.1. *Chemistry*

The chemistry of the data is surprising. Again, the observations were toward Sgr A* and we expect significant contributions from the GC. However, many of our clouds only contain CO isotopologues. We essentially see fewer molecules and transitions in our clouds than we expected, and so the judgement of "chemically rich" is relative to the clouds in our data rather than our expectations of clouds in the GC. This may indicate that the dense gas that the chemical lines are sensitive to are colder than expected, or perhaps isolated and clumpy which can cause more variations on even neighboring sightlines.

We define a chemically rich cloud as one that contains molecular lines other than CO isotopologues. The $+10.75$ km s^{-1} feature is our most chemically rich cloud with significant detections ($\tau > 3\sigma$) of all molecular lines in Table 1 except for N_2D^+, $C^{15}N$, and NH_2D. This cloud also contains dense gas tracers such as CS. The chemistry of the $+10.75$ km s^{-1} cloud indicates that it is our best candidate for an inner GC cloud, perhaps somewhere in the central CMZ.

The -55 km s^{-1} feature is our next chemically rich cloud, with detections of C_2H and o-NH_2D or p-NH_2D in addition to ^{12}CO, ^{13}CO, and $C^{18}O$. The -13 km s^{-1} cloud contains similar detections except for NH_2D. Despite being our second and third most chemically rich features, these clouds only contain one or two other detections besides CO isotopologues rather than many. It

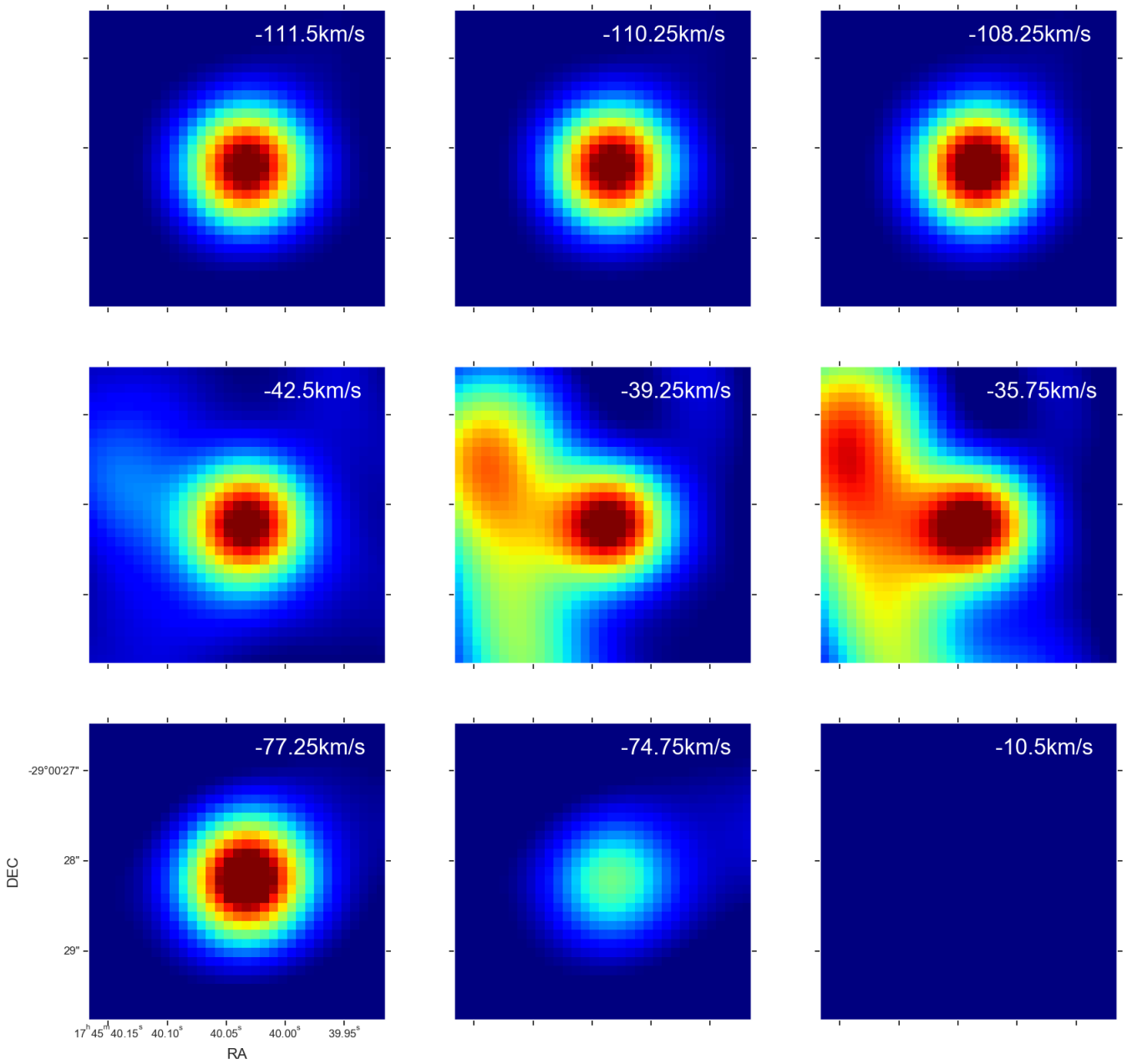

Figure 1: Select channels from the ^{12}CO(3-2) data cube featuring examples of continuum emission (top row), emission (middle row), and absorption (bottom row). The bottom right panel at -10.5 km s^{-1} features total absorption down to 0 Jy bm^{-1}.

appears as though these clouds may be somewhere in the inner Galactic Disk when analyzing this chemistry.

The $+42.5$ km s^{-1} and -33 km s^{-1} clouds are not chemically rich with detections of just ^{12}CO, ^{13}CO, and C^{18}O. Chemistry alone suggests that the clouds are somewhere in the Galactic Disk rather than in the chemically-rich GC, though these are not final designations due to other factors that will be discussed, such as kinematics and CO isotopologue ratios.

3.3.2. *CO Ratios*

For each cloud, we calculate a ^{12}CO(3-2)/^{12}CO(2-1) opacity ratio in order to understand its excitation. A higher excitation cloud, or one that contains more ^{12}CO(3-2) opacity than ^{12}CO(2-1) opacity, will return a value ≥ 1. A cloud with lower excitation will return a value < 1. This is because the ^{12}CO(3-2) transition involves higher J excitation states than the ^{12}CO(2-1) transition.

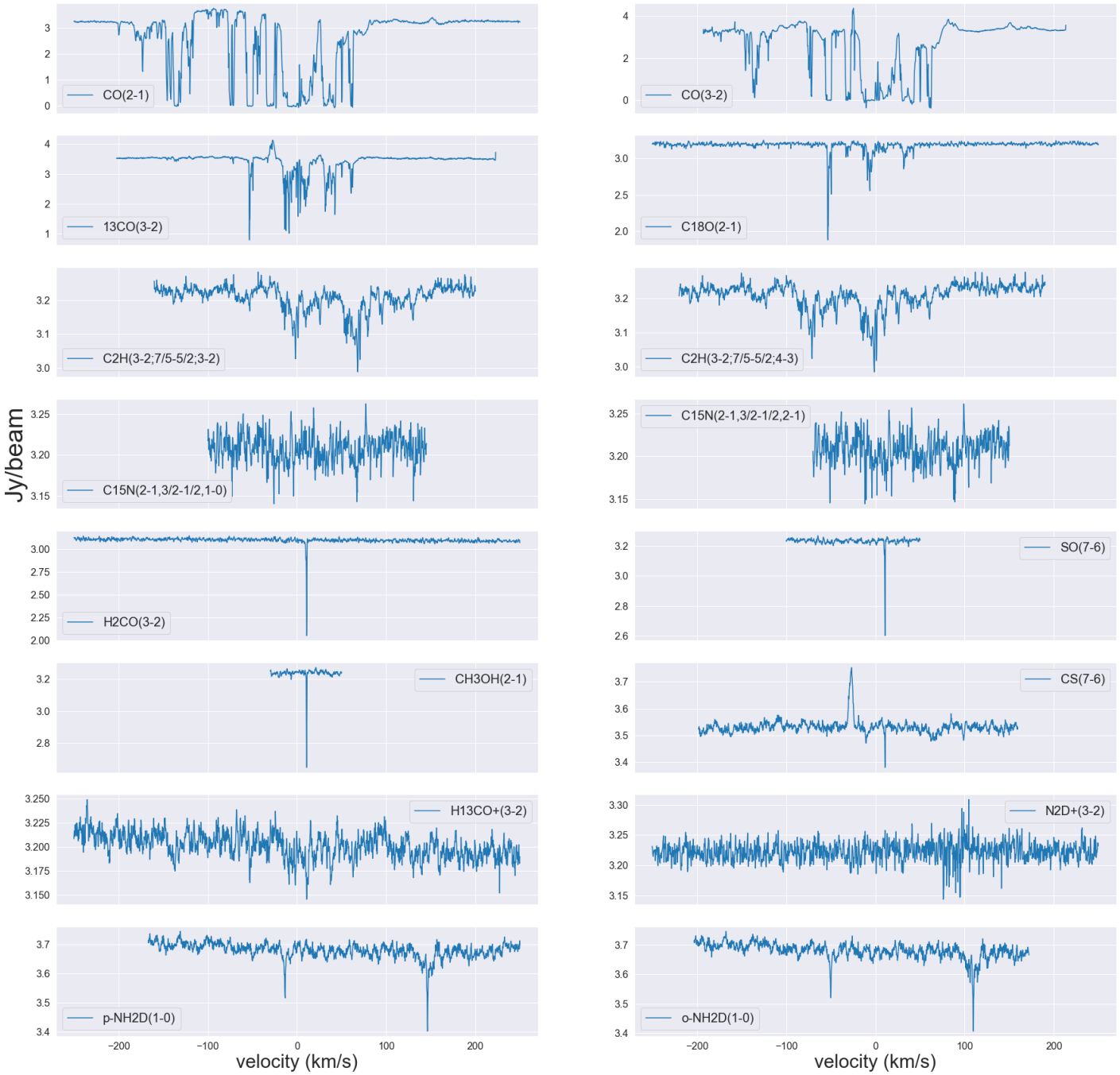

Figure 2: Spectral profiles of the molecules and transitions in our data. The y-axis is flux density in Jy bm^{-1} and the x-axis is velocity in km s^{-1}. Large upward spikes in C_2H, $C^{15}N$, and N_2D^+ are due to artifacts in the data cubes and have been trimmed from the spectra. SiO is not included due to no clear detections in its spectrum, and HNCO has also been excluded due to the presence of atmospheric lines. It is currently unclear whether there are actual detections of $C^{15}N$ and N_2D^+. The features in both NH_2D spectra have not been properly identified.

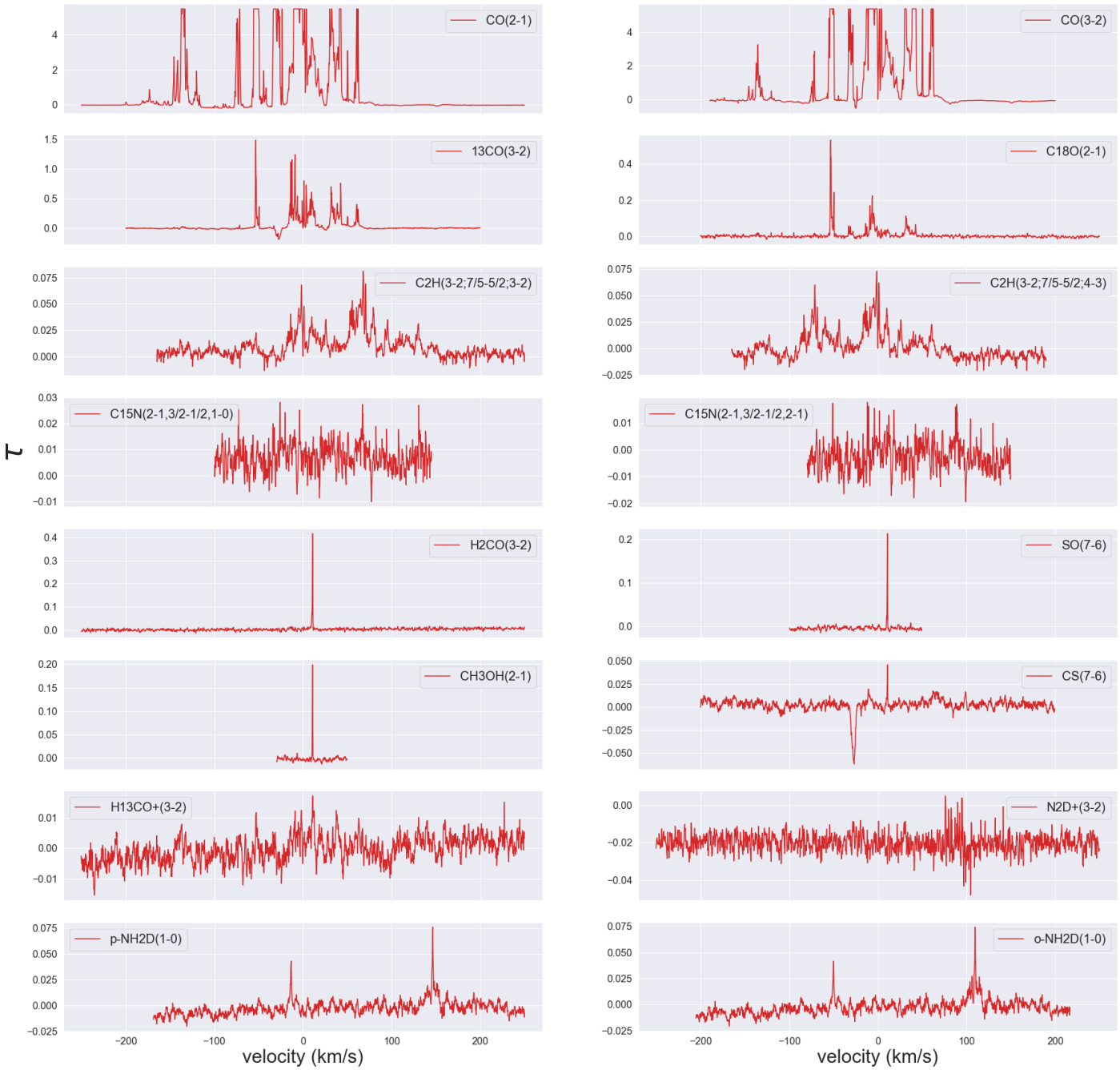

Figure 3: Spectral profiles in opacity space, where the y-axis is the dimensionless number τ and the x-axis is velocity in km s^{-1}. The spectra have been trimmed to only show relevant features, as explained in Figure 2. The ^{12}CO and ^{13}CO profiles contain many instances of absorption down to 0 Jy bm^{-1}, or completely opaque clouds, as indicated by the "flat tops" of the spectra.

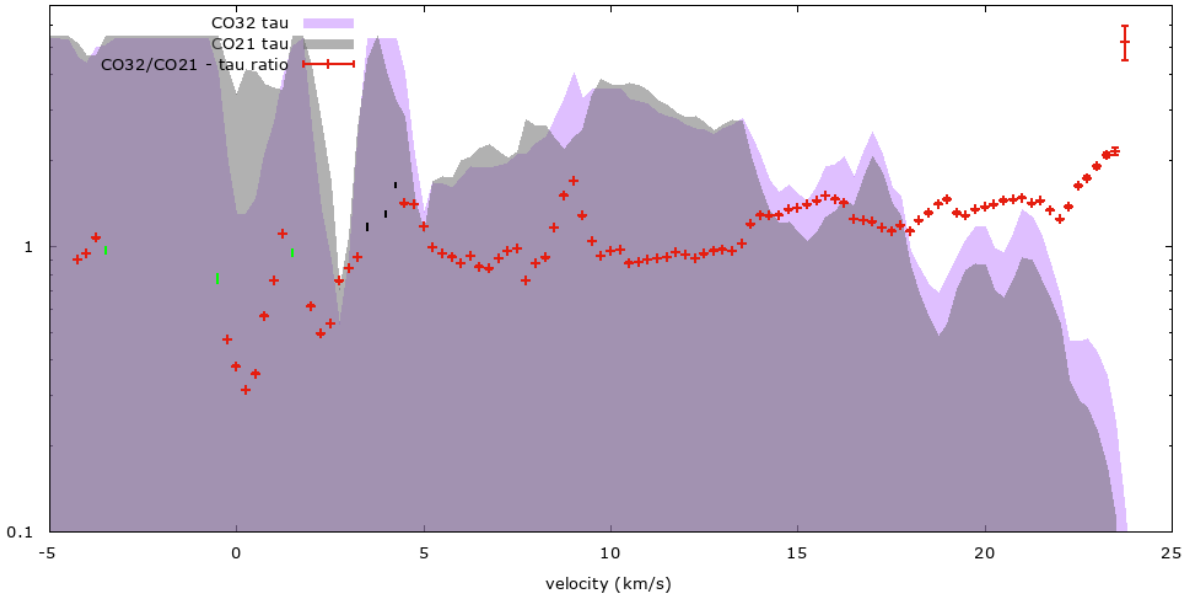

Figure 4: ^{12}CO(3-2)/^{12}CO(2-1) ratio for velocities between -5 km s^{-1} and $+25$ km s^{-1}. The ^{12}CO(3-2) opacity spectrum is represented by the light purple shading, while the gray shading is the ^{12}CO(2-1) opacity spectrum. The dark purple is where the two spectra overlap. The red tick marks are the measured ^{12}CO(3-2)/^{12}CO(2-1) ratio values. The green marks indicate upper limits, whereas the black marks indicate lower limits. Higher excitation and warm gas ($T \gtrsim 15$ K) results in a value ≥ 1.

The excitation of a cloud also provides clues as to its temperature, where higher excitation indicates a warmer cloud ($T \gtrsim 15$ K). Higher temperatures hint at the physics of the cloud, such as the presence of shocks, feedback, or protostellar activity in the molecular material. We expect these kinds of physical conditions to be consistent with the hot, dense environment of the GC.

Figure 4 is a visualization of the ^{12}CO(3-2)/^{12}CO(2-1) ratio for a velocity range of -5 km s^{-1} to $+25$ km s^{-1}. The red marks are the measured ratio values. For our $+10.75$ km s^{-1} cloud, the ratio values are $\sim$1, indicating that our most chemically-rich cloud also has moderately high excitation. Thus the $+10.75$ km s^{-1} cloud is most likely made up of warm material ($T \gtrsim 15$ K). This is consistent with the fact that we see the richest warm cloud chemistry here.

Our -135 km s^{-1} and -55 km s^{-1} clouds return ^{12}CO(3-2)/^{12}CO(2-1) ratio values < 1. These clouds appear to have lower excitation and thus colder temperatures ($T \lesssim 15$ K). The -33 km s^{-1} cloud has a value only slightly < 1, indicating only moderately low excitation with a cooler temperature. Much like the $+10.75$ km s^{-1} cloud, the -13.25 km s^{-1} cloud has a value slightly > 1, or is moderately excited with warmer temperatures. The $+42.5$ km s^{-1} cloud has high excitation with hotter temperatures, as indicated by its ^{12}CO(3-2)/^{12}CO(2-1) ratio value > 1.

We next calculate a ^{12}CO(3-2)/^{13}CO(3-2) ratio, which is indicative of Galactocentric radius. Wilson & Rood (1994) cite a ^{12}CO/^{13}CO value of $\sim$25 for the GC and $\sim$75 for the Galactic Disk. A lower ratio value corresponds to the GC because we expect more generations of stars, and thus more isotopes, to be present in the GC. Figure 5 shows the ^{12}CO/^{13}CO ratio for our -5 km s^{-1} to $+25$ km s^{-1} region. This plot shows that our $+10.75$ km s^{-1} cloud has a ^{12}CO/^{13}CO value < 25, supporting the idea that this cloud is in the GC.

The -13.25 km s^{-1} and $+42.5$ km s^{-1} return similar ^{12}CO/^{13}CO ratio values to the $+10.75$ km s^{-1} cloud. The ratio for the -55 km s^{-1} cloud is only slightly $<$ 25, suggesting it is in the GC but not as GC-like as the -13.25 km s^{-1}, $+10.75$ km s^{-1}, and $+42.5$ km s^{-1} features. The -135 km s^{-1} and -33 km s^{-1} clouds return ratios above the $\sim$75 Galactic Disk value ($\sim$100 and > 200, respectively), suggesting that these clouds are located outside the GC and in the disk.

Finally, we take a ^{12}CO/C^{18}O ratio, another indicator of Galactocentric distance. Wilson & Rood (1994) cite a ^{12}CO/C^{18}O value of $\sim$200 for the GC and $\sim$500 for the Galactic Disk. The $+10.75$ km s^{-1} cloud returns a ratio value slightly < 200, suggesting the cloud is in the GC and further supporting the ^{12}CO/^{13}CO ratio results (Figure 6).

The $+45.2$ km s^{-1} cloud returns similar results to the $+10.75$ km s^{-1} material. Both the -55 km s^{-1} cloud

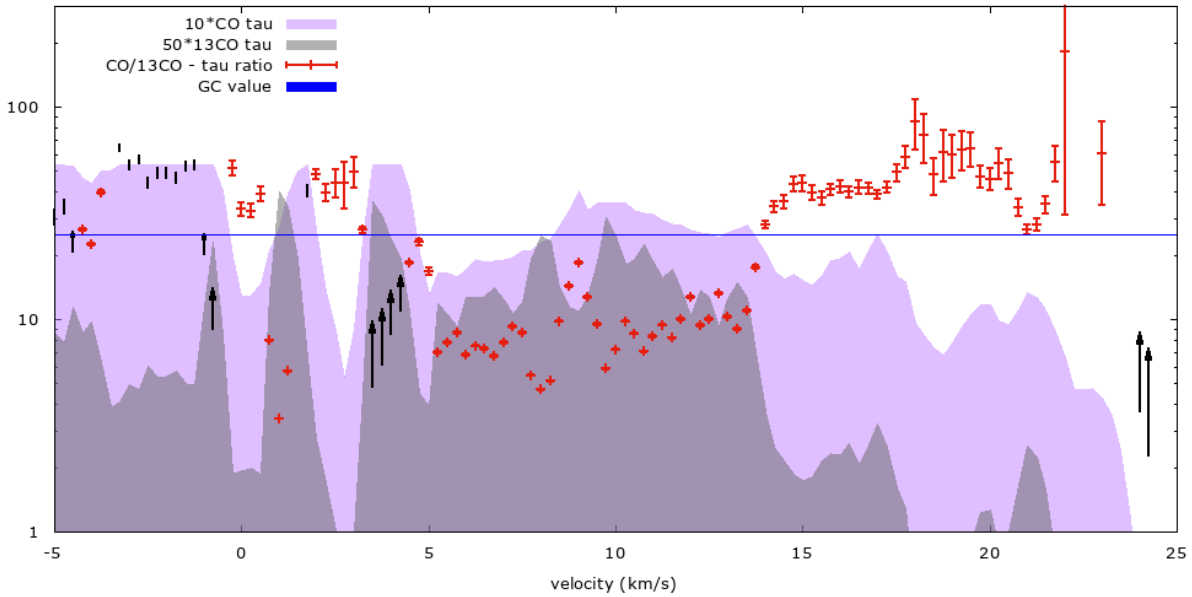

Figure 5: ^{12}CO(3-2)/^{13}CO(3-2) ratio for velocities between -5 km s^{-1} and $+25$ km s^{-1}. The ^{12}CO opacity spectrum is represented by the light purple shading, while the gray shading is the ^{13}CO opacity spectrum. Both are multiplied by a scalar so they fit onto one plot. The overlap between the two is represented by the dark purple spectrum. The red tick marks are the measured ^{12}CO/^{13}CO ratio values, and the black marks indicate lower limits. The horizontal blue line is the GC ratio value of 25. Any value $\lesssim 25$ suggests the cloud is towards the GC.

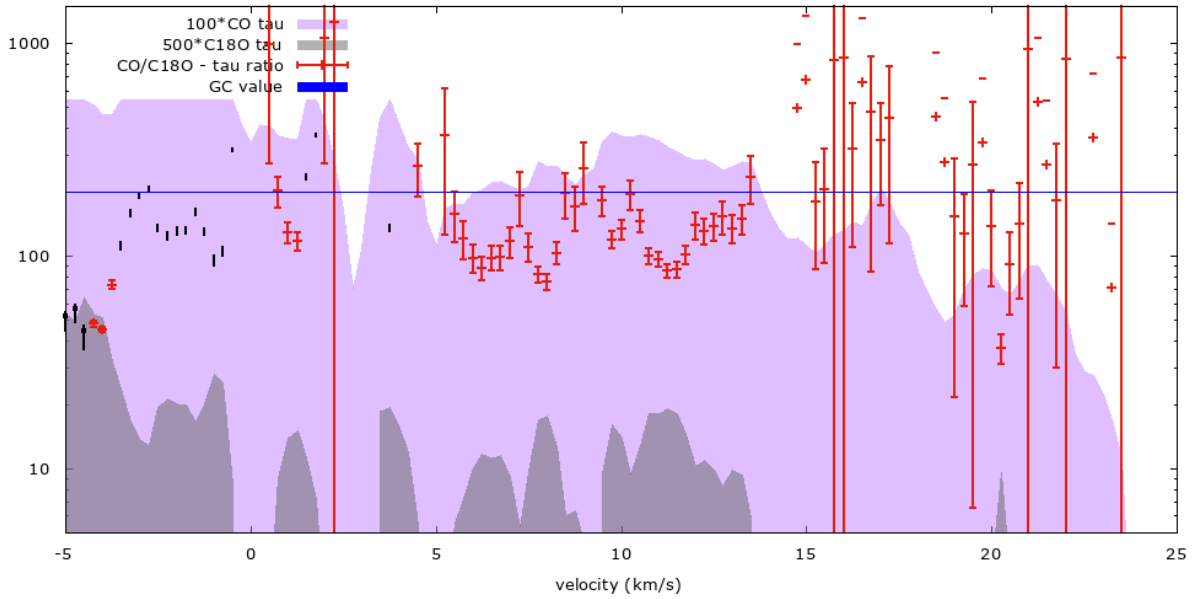

Figure 6: ^{12}CO(2-1)/C^{18}O(2-1) ratio for velocities between -5 km s^{-1} and $+25$ km s^{-1}. The ^{12}CO opacity spectrum is represented by the light purple shading, while the gray shading is the C^{18}O opacity spectrum. Both are multiplied by a scalar so they fit onto one plot. The overlap between the two is represented by the dark purple spectrum. The red tick marks are the measured ^{12}CO/C^{18}O ratio values, and the black marks indicate lower limits. The horizontal blue line is the GC ratio value of 200. Any value $\lesssim 200$ suggests the cloud is towards the GC.

and −13.25 km s^{-1} cloud contain ratio values < 200, which supports the ^{12}CO/^{13}CO results, suggesting that these are in the GC. We obtain Galactic Disk-like values for the −135 km s^{-1} and −33 km s^{-1} clouds (much higher than 200 and slightly < 500, respectively). These Galactic Disk values are consistent with the values we obtain for the ^{12}CO/^{13}CO ratio.

The ^{12}CO/C^{18}O ratio appears to support the results of the ^{12}CO/^{13}CO ratio for all of our clouds. The Galactocentric distance ratios alone suggest that the −13.25 km s^{-1}, +10.75 km s^{-1}, and +42.5 km s^{-1} clouds are good candidates for GC material. The −135 km s^{-1}, −55 km s^{-1}, and −33 km s^{-1} clouds appear to be somewhere in the Galactic Disk. The excitation ratios support this for all clouds except the −55 km s^{-1} feature, whose ^{12}CO(3-2)/^{12}CO(2-1) ratio describes the cloud as low excitation with colder temperatures. We expect warmer clouds with higher excitation to be located in the GC, and so the excitation ratio and the Galactocentric distance ratios appear to disagree for the material at −55 km s^{-1}.

3.3.3. *Kinematics*

We use the position-velocity (PV) diagram from Stark et al. (2004) to study the kinematics of these clouds (Figure 7). In the context of bar models, the position of Sgr A* is located at 0 degrees Galactic longitude on the x-axis. This PV diagram is the volume density of CO based on non-LTE single zone radiative transfer calculations. Thus, we look at the density of material around 0 degrees to see if molecular material at certain velocities can be in the GC or even near Sgr A*.

We note that there is dense +10.75 km s^{-1} and +42.5 km s^{-1} molecular material around 0 degrees. This also appears to be the case for our −13.25 km s^{-1} cloud, though Greaves & Williams (1994) claim material at this velocity would be in the 4 kpc arm of the bar. Dense −55 km s^{-1} and −33 km s^{-1} molecular material is also present around 0 degrees, though perhaps not exactly around Sgr A*. Greaves & Williams (1994) disagree with this assessment of the −33 km s^{-1} cloud, suggesting that it should be in the 3 or 4 kpc arm based on their own study of GC velocity gas. For the −135 km s^{-1} cloud, Greaves & Williams (1994) appear to agree with the Stark et al. (2004) model, indicating that the material is most likely around the 3 kpc arm based on the presence of dense molecular material there at about the same velocity. All clouds could be located in the GC if we fully adopt the Stark et al. (2004) model.

4. DISCUSSION

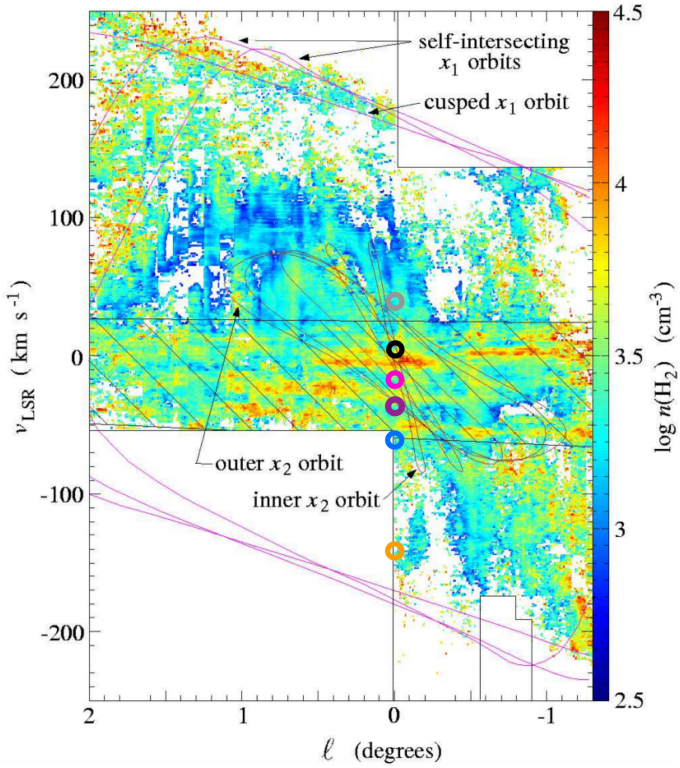

Figure 7: Position-velocity diagram adopted from Stark et al. (2004). The y-axis is velocity in km s^{-1} and the x-axis is in degrees, where 0 is the location of Sgr A*. Stark et al. (2004) describe the color bar as representing the density of the molecular material. The bottom pink lines are about the location of the 3 kpc arm of the Galactic bar, and the horizontal stripes are disk material. The molecular material at each velocity at 0 degrees is marked with a circle: gray for +42.5 km s^{-1}, black for +10.75 km s^{-1}, pink for −13.25 km s^{-1}, purple for −33 km s^{-1}, blue for −55 km s^{-1}, and orange for −135 km s^{-1}.

The following discussion will detail the reasoning behind our current cloud identifications (see Table 2 for a summary).

4.1. *Galactic Center Clouds*

The placement of the +10.75 km s^{-1} cloud along our line-of-sight is perhaps the most straight forward. Its molecular material is chemically rich with moderately high excitation and thus warmer temperatures. The CO isotopologue ratios and kinematics suggest that the cloud is in the GC. All of these factors point toward the +10.75 km s^{-1} cloud being in the GC. We note the velocity of this cloud is similar to the +20 km s^{-1} cloud in the 100 pc ring of the CMZ. It is probable that this

Table 2: Summary of our cloud identifications.

Cloud	CO(3-2)/ CO(2-1)	12CO(2-1)/ C18O(2-1)	CO(3-2)/ 13CO(3-2)	Chemistry	Kinematics	ID
-135 km/s	<1	>>200	∼100	not chemically rich	3 kpc arm inwards	Inner Galaxy
-55 km/s	<1	<<200	slightly <25	chemically rich (NH2D and C2H)	GC	Intermediate Inner Galaxy/outer GC
-33 km/s	slightly <1	slightly <500	>200	not chemically rich	3 or 4 kpc arm	Galactic Disk, maybe 3 kpc arm
-13.25 km/s	slightly >1	<200	<25	somewhat chemically rich (C2H)	4 kpc arm	?????
+10.75 km/s	slightly >1	slightly <200	<25	most chemically rich; dense gas tracers	GC	GC; maybe 100 pc ring
+42.5 km/s	>1	slightly <200	<25	not chemically rich	GC	GC; maybe 100 pc ring

cloud is also in the 100 pc ring, perhaps even being a residual of the +20 km s^{-1} cloud itself.

The +42.5 km s^{-1} cloud is also one we place in the GC. It has high excitation and thus hotter temperatures. The CO isotopologue ratios and kinematics suggest the cloud is in the GC. However, the material at +42.5 km s^{-1} is not chemically rich with only CO isotopologues detected. This is surprising because we expect clouds in the GC to be chemically rich. Further, +42.5 km s^{-1} is a velocity similar to the +50 km s^{-1} cloud that is in the 100 pc ring of the CMZ. It is possible our +42.5 km s^{-1} cloud is also in the 100 pc ring and may even be a residual of the +50 km s^{-1} cloud, much like our reasoning for the +10.75 km s^{-1} cloud. Despite the +42.5 km s^{-1} being not very chemically rich, we designate it as a GC cloud with the possibility of being in the 100 pc ring of the CMZ due to its kinematics and CO isotopologue ratios.

4.2. *Galactic Disk Clouds*

We place the −135 km s^{-1}, −55 km s^{-1}, and −33 km s^{-1} clouds in the Galactic Disk. Of these, the −33 km s^{-1} cloud is the easiest to place. It is not chemically rich with lower excitation and thus colder temperatures. Its CO isotopologue ratios return Galactic Disk-like values. Kinematically, the cloud is consistent with material in the arms of the bar. Thus, we place the −33 km s^{-1} cloud in the Galactic Disk, perhaps in the 3 kpc arm.

The −55 km s^{-1} cloud is our second-most chemically rich cloud and kinematically could be in the GC, which is interesting because all other factors point toward the cloud being in the Galactic Disk. It has lower excitation, lower temperatures, and CO isotopologue ratio values that are Galactic Disk-like. Because of these discrepancies, we do not believe the cloud is in the GC, though it is most likely close. We designate this cloud as being in the intermediate Inner Galaxy, or the outer edge of the GC.

The −135 km s^{-1} cloud is interesting due to its kinematics. It is not chemically rich, has low excitation, and is thus made of colder material. Its CO isotopologue ratios return high Galactic Disk-like values, suggesting it is way out in the disk. However, Figure 7 places the cloud closer to the GC than anticipated, being somewhere around the 3 kpc. These conflicting results lead us to designating the cloud as being somewhere in the Inner Galaxy. It is possible that this cloud is a recently accreted disk cloud.

4.3. *The −13.25 km s^{-1} Cloud*

We are unable to properly place the −13.25 km s^{-1} cloud along our line-of-sight toward Sgr A*. Based on its kinematics and somewhat chemically-rich nature, it appears as though the cloud could be towards the GC. The CO isotopologue and excitation ratios appear to agree with this assessment. However, we cannot place emphasis on these ratios. At −13.25 km s^{-1}, the ^{12}CO spectra have "flat tops." In other words, the cloud at −13.25 km s^{-1} is so opaque in ^{12}CO that our data is saturated and the ratios become poorly constrained. Because of

this, we cannot interpret the CO isotopologue ratios as well as we could for the other clouds. Thus, we leave the material at -13.25 km s^{-1} as an unknown cloud somewhere along our line-of-sight.

5. CONCLUSIONS

We analyze absorption features along the line-of-sight to Sgr A* using ALMA data. We detect 16 molecular lines from 12 molecules in clouds along this line-of-sight. We summarize 6 notable clouds and place them in either the Galactic Disk or GC via kinematics, chemistry, excitation, and CO isotopologue ratios (Galactocentric distance).

We do not have a current candidate for a CND cloud. However, the material at $+10.75$ km s^{-1} is most likely the closest cloud to the environment of Sgr A*, being somewhere around the 100 pc ring of the CMZ. The $+42.5$ km s^{-1} cloud could also be in the 100 pc ring, though its chemistry suggests it is not as deep in the GC. The -55 km s^{-1} and -33 km s^{-1} clouds are consistent with Galactic Disk clouds, but still reside somewhere in the Inner Galaxy. The material at -135 km s^{-1} is interesting due to its kinematics suggesting that it is in the Inner Galaxy rather than the Galactic Disk, which all other factors appear to point to. The -13.25 km s^{-1} cloud is unable to be understood via CO isotopologue ratios, and thus its location in our Galaxy remains unknown.

The next goal of our project is to unveil a candidate cloud for the CND. As noted in Section 3, we see many emission features in our ^{12}CO and CS spectral profiles. These emission features will likely reveal a cloud in the hot CND. More work is also needed to be done with our current absorption data. We will inspect 3 mm ALMA data in hopes of finding more bright lines. We must also investigate unknown lines, such as the bright absorption features in the NH_2D spectrum, in order to properly identify them. Calculating abundance ratios and column densities will also play a role in fully understanding these clouds.

ACKNOWLEDGMENTS

We acknowledge support from the National Science Foundation Research Experience for Undergraduates (REU) program at the National Radio Astronomy Observatory in Socorro, New Mexico. This paper makes use of the following ALMA data: ADS/JAO.ALMA#2012.1.00628.T. ALMA is a partnership of ESO (representing its member states), NSF (USA) and NINS (Japan), together with NRC (Canada), MOST and ASIAA (Taiwan), and KASI (Republic of Korea), in cooperation with the Republic of Chile. The Joint ALMA Observatory is operated by ESO, AUI/NRAO and NAOJ. The National Radio Astronomy Observatory is a facility of the National Science Foundation operated under cooperative agreement by Associated Universities, Inc. We thank the ALMA NAASC data reduction group for calibration of the data.

Software: CASA (McMullin et al. 2007), Jupyter (Kluyver et al. 2016), Astropy (Astropy Collaboration et al. 2013; Price-Whelan et al. 2018), pandas (McKinney et al. 2010), NumPy (Van Der Walt et al. 2011), Seaborn (Waskom et al. 2017), Matplotlib (Hunter 2007)

Facilities: ALMA

REFERENCES

Astropy Collaboration, Robitaille, T. P., Tollerud, E. J., et al. 2013, A&A, 558, A33, doi: 10.1051/0004-6361/201322068

Gravity Collaboration, Abuter, R., Amorim, A., et al. 2019, A&A, 625, L10, doi: 10.1051/0004-6361/201935656

Greaves, J. S., & Williams, P. G. 1994, A&A, 290, 259

Hunter, J. D. 2007, Computing in Science & Engineering, 9, 90, doi: 10.1109/MCSE.2007.55

Kluyver, T., Ragan-Kelley, B., Pérez, F., et al. 2016, in ELPUB, 87–90

McKinney, W., et al. 2010, in Proceedings of the 9th Python in Science Conference, Vol. 445, Austin, TX, 51–56

McMullin, J. P., Waters, B., Schiebel, D., Young, W., & Golap, K. 2007, in Astronomical Society of the Pacific Conference Series, Vol. 376, Astronomical Data Analysis Software and Systems XVI, ed. R. A. Shaw, F. Hill, & D. J. Bell, 127

Molinari, S., Bally, J., Noriega-Crespo, A., et al. 2011, ApJL, 735, L33, doi: 10.1088/2041-8205/735/2/L33

Morris, M., & Serabyn, E. 1996, ARA&A, 34, 645, doi: 10.1146/annurev.astro.34.1.645

Price-Whelan, A. M., Sipőcz, B. M., Günther, H. M., et al. 2018, AJ, 156, 123, doi: 10.3847/1538-3881/aabc4f

Stark, A. A., Martin, C. L., Walsh, W. M., et al. 2004, ApJL, 614, L41, doi: 10.1086/425304

Van Der Walt, S., Colbert, S. C., & Varoquaux, G. 2011, Computing in Science & Engineering, 13, 22

Waskom, M., Botvinnik, O., O'Kane, D., et al. 2017, doi: 10.5281/zenodo.883859

Wilson, T. L., & Rood, R. 1994, ARA&A, 32, 191, doi: 10.1146/annurev.aa.32.090194.001203